

Effect of anorthite liquid on the abnormal grain growth of alumina

Sang-Ho Lee^a, Doh-Yeon Kim^{a,*}, Nong M. Hwang^b

^aCenter for Microstructure Science of Materials and School of Materials Science and Engineering,
Seoul National University, Seoul 151-742, South Korea

^bKorea Research Institute of Standards and Science, Taejon 305-340, South Korea

Received 16 November 2000; accepted 26 March 2001

Abstract

A small amount of anorthite ($2\text{CaO}\cdot\text{Al}_2\text{O}_3\cdot\text{SiO}_2$) powder was placed on the top-center of the pure Al_2O_3 powder compact and then sintered at 1600°C . During sintering some grains grew extensively along the radial direction from the liquid source. By considering an atomically smooth solid–liquid interface structure of alumina, grain growth controlled by 2-dimensional (2-D) nucleation was suggested. The elongation has been explained in terms of nucleation advantage of grain-boundary re-entrant edges (GBRE) formed dominantly at non-basal planes. © 2001 Elsevier Science Ltd. All rights reserved.

Keywords: Al_2O_3 ; Grain growth; Microstructure-final; Sintering

1. Introduction

Abnormal grain growth (AGG) during sintering of alumina^{1–7} is generally due to the liquid forming impurities such as CaO , SiO_2 and TiO_2 . In the high purity alumina, indeed, it was hard to observe AGG even after sintering at 1900°C .⁸ Furthermore, abnormally grown alumina grains always exhibit well developed basal planes with a thin intergranular film.^{9–12} On the other hand, Kolar¹³ suggested that the uneven distribution of a small amount of liquid, which brings about the coexistence of wet and dry boundaries, is the primary cause of AGG.

It should be noted, however, that AGG in the presence of liquid is a phenomenon only observed when the grains are angular with flat interfaces. WC-Co ,^{14,15} BaTiO_3 ,^{16,17} Si_3N_4 ,^{18,19} SiC ,²⁰ mullite²¹ and B_4C ²² are typical examples of angular grains which exhibit AGG. When the grains are spherical, such as W-Ni ²³ and MgO-CaMgSiO_4 ,²⁴ no AGG is observed to occur. Such a shape dependence of a coarsening behavior has been explained^{25–30} in terms of the atomic structure of the solid–liquid interface.

When the grains are spherical, the interface structure is atomically rough. In this case, atomic attachment to

the interface has a negligible energy barrier so that the coarsening process is controlled by diffusion through the liquid. For angular grains with atomically smooth interfaces, on the contrary, the ledge-generating sources such as 2-dimensional (2-D) nucleation are necessary for the atomic attachment. Due to significant energy barrier for 2-D nucleation, only very large grains having enough driving force for coarsening can grow. This process has been suggested to be the mechanism of AGG.^{15,17–19,25–30}

In fact, Herring³¹ has suggested that the facet planes would show a discontinuous variation in growth behavior if coarsening by 2-D nucleation were involved. Furthermore, Wynblatt et al.^{32,33} have shown that the growth of faceted Pt particles on alumina substrates is “nucleation inhibited”. Although they did not explicitly mention the AGG behavior, their works are believed to lay a base for the 2-D nucleation controlled coarsening process which leads to AGG.

The flat basal plane of abnormally grown alumina grains in the presence of liquid is the direct evidence of an atomically smooth solid–liquid interface. In this investigation, therefore, we examined AGG in alumina on the basis of a 2-D nucleation mechanism. To obtain the microstructure with various liquid concentrations at a same time, a small amount of anorthite composition

* Corresponding author. Fax: +82-2884-1413.
E-mail address: dykim@snu.ac.kr (D.-Y. Kim).

($2\text{CaO} + \text{Al}_2\text{O}_3 + \text{SiO}_2$) powder was placed on top of an alumina powder compact. A gradient in liquid concentration was expected to develop in the specimen. The grain boundary re-entrant edge (GBRE) formed at non-basal planes of alumina was suggested to cause an exceptional and anisotropic growth. As observed in NbC–Fe²⁹ and TaC–TiC–Ni³⁰ systems, the growth is accelerated when the grain boundaries are formed because the energy barrier for 2-D nucleation is markedly reduced at the re-entrant edges.

2. Experimental procedure

Alumina powder (purity 99.995%, average particle size 0.4–0.7 μm , AKP 3000, Sumitomo Chemicals Ltd, Osaka, Japan) with impurity levels of Si, Na, Mg, Cu and Fe of 20, 10, 10, 10 and 10 ppm, respectively, was used. Two grams of the powder was slightly compacted into a cylindrical specimen 15 mm in diameter and then pressed hydrostatically at 150 MPa. The anorthite powder mixture ($2\text{CaO} + \text{Al}_2\text{O}_3 + \text{SiO}_2$ in mole ratio) was prepared by using CaCO_3 (Yakuri Pure Chemicals, 1st grade, Osaka, Japan), pure Al_2O_3 (AKP 3000) and SiO_2 (purity 99%, Sigma Chemical Co., St Louis, USA) powders.

At the center of the top surface of the powder compact, a very small amount of anorthite powder (less than 0.01 g) was placed. The compact was then calcined at 900°C for 30 m and sintered at 1600°C for up to 24 h. The anorthite powder mixture became a point liquid source during sintering and penetrated into the alumina powder compact. The liquid concentration was expected to have a gradient along the distance from the source. The sintered specimens were cut along the diameter and the vertical cross-sections were polished. The specimens were observed by optical and scanning electron microscopy after thermal etching at 1550°C for 30 m. Electron probe microanalysis (EPMA) was carried out to determine the liquid distribution.

3. Results and discussions

The microstructure of the specimen after sintering at 1600°C for 0.5 h is shown in Fig. 1(a). It shows the region near the point of liquid source. The liquid formed at the top surface of the specimen has completely penetrated into the alumina. However, the presence of liquid was rather limited at the specimen surface (about 500 μm in depth). It is probably due to the dihedral angle which is greater than zero and consequent entrapment of liquid at the triple boundary junctions. High viscosity of liquid may also be the reason. Note from Fig. 1(a) that the microstructure of the surface region affected by liquid has much larger grains compared to that of the interior. A small number of

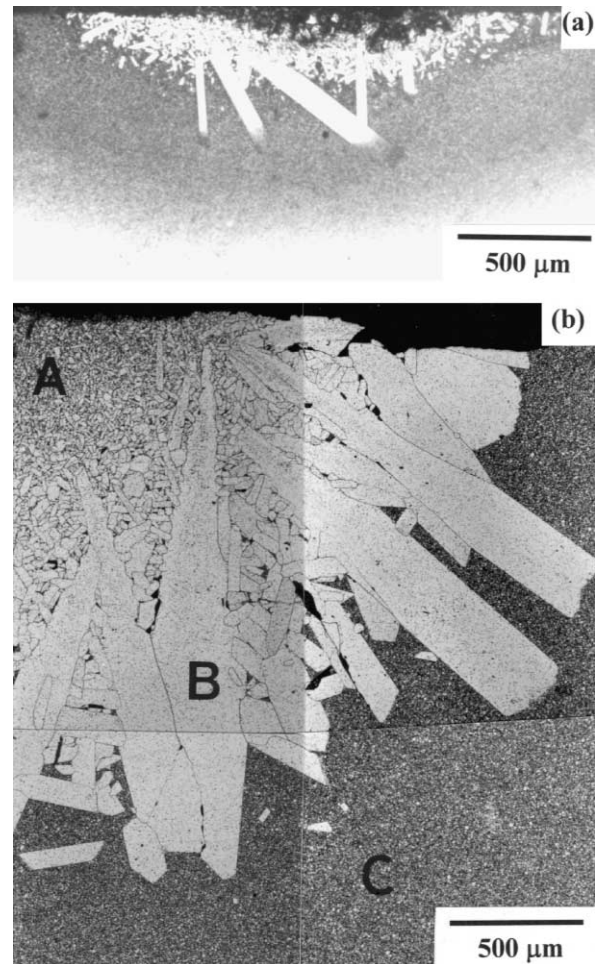


Fig. 1. Microstructures of the Al_2O_3 specimens sintered at 1600°C for (a) 0.5 h and (b) 24 h.

elongated very large grains (length and width up to around 800 and 100 μm , respectively) were also observed to appear.

Fig. 1(b) is the microstructure of the same specimen obtained after the heat-treatment for 24 h. It shows the right-hand half of the cross-section; the left-hand half was almost identical. This microstructure of the surface region up to about 2500 μm in depth is quite unusual with extensively grown abnormal grains. The elongated grains with their lengths in the radial direction from the liquid source strongly indicate that the anorthite liquid plays an important role in the growth process.

For Fig. 1(b), three separate regions of different grain sizes and shapes can be defined depending on the distance from the liquid source. In the region close to the liquid source (region A), the grains are relatively large and uniform in size distribution. Within the region, however, the increase in average grain size with increasing distance from the liquid is noted. In the second region (region B), the grains become much larger and elongated. This region starting 0.5–1 mm away from the liquid source shows a typical microstructure of

AGG. The average size of grains was ~ 2000 and ~ 300 μm in length and width, respectively. The third region (region C) may represent the microstructure which was unaffected by the liquid. In this region the grains are again uniform in size and equiaxed. The average size of grains was 10.5 μm , which is much finer than that of region A. In fact, the microstructure of region C was practically the same as that of the pure alumina specimen prepared without any liquid.

The microstructures shown in Fig. 1 clearly indicate that grain growth is enhanced by the presence of liquid. However, it should be noted that the grain size increased with the distance from the liquid source i.e. with the decrease of liquid content. In Fig. 1(b), for instance, an appreciable amount of liquid was observed to exist in the region A, but the liquid was almost absent in the region C. Such radial concentration gradient of the liquid was also checked through the area composition analysis of Ca by using EPMA. The concentration of Ca in region A (0.038 wt.%), approximately 0.1 mm away from liquid source, was determined to be much higher than that of the region C (0.009 wt.%). In this respect, the difference in microstructure is believed to be due to the concentration gradient of the anorthite liquid.

The enhanced grain growth by the presence of liquid implies that the mobility of the liquid film is higher than that of the grain boundary. Note that the rate of material transfer across the liquid film is higher than that across the grain boundary. Variation of grain size observed in Fig. 1(b) can also be related with the high mobility of liquid film. The further the distance from the liquid source, the lower the liquid content as well as the fraction of liquid film. In this case, the number of grains that can grow by liquid film migration becomes smaller and consequently a larger average grain size is obtained. In this respect, AGG that appeared in region B is likely to be due to a very limited liquid content. When the overall liquid content becomes lower than a certain limit, only a few grains are expected to grow extensively.

For abnormally grown elongated alumina grains in region B, the basal surface is flat and the non-basal surface is mixed with curved and flat areas, as revealed in the detailed microstructure of Fig. 2. As reported by Kooy,³⁴ the appearance of flat boundaries indicates the presence of a continuous liquid phase at the boundaries. Otherwise, the interface with various curvatures would appear due to randomly oriented small matrix grains. From Fig. 2 and observations using TEM,^{9–12} it is believed that both a liquid film and grain boundary are present at the interface of non-basal plane while the liquid film is present at almost the entire interface of the basal plane.

On the other hand, it is predicted from the aspect ratio of abnormally grown elongated grains that the mobility of the non-basal plane is about 7 times higher than that of the basal planes. Due to such fast migration

of non-basal plane, not only the pores but also the grains (indicated by an arrow in Fig. 2) were trapped. This observation poses an interesting question: how the partially wetted non-basal planes migrate at a rate much higher than fully wetted basal planes? In order to answer this question, the mechanism of material transfer across the liquid film, which is dependent on the atomic structure of the solid–liquid (S/L) interface should first be considered.

The atomic structure of the S/L interface is either smooth or rough. One of the theoretical criteria for smooth and rough interfaces is Jackson's α parameter.³⁵ The S/L interface of metallic systems tends to be rough while that of ceramic systems tends to be smooth. Normally, the S/L interface structure can be easily determined by observing an equilibrium or a near-equilibrium shape of the grain, which is developed when the solid grains are dispersed in a liquid matrix of sufficient amount. The shape of alumina grains in such a condition is quite angular,^{6,12,36–38} which indicates that the S/L interface of alumina is atomically smooth. The flatness of the basal surface of alumina as shown in Figs. 1 and 2 may also be an indication of a smooth atomic structure of the interface.

Atomic attachment to a smooth interface occurs typically by 2-D nucleation and lateral growth mechanism. On the other hand, it has been reported that the barrier for 2-D nucleation is reduced markedly when the re-entrant edges made by a twin^{16,17,28} or a grain boundary^{29,30} are present. Fig. 3(a) and (b) shows the schematic diagram showing a comparison of 2-D nucleation at terrace and the re-entrant edge, respectively.

When a cylindrical monoatomic layered nucleus is formed on the terrace plane, the nucleation barrier is expressed as

$$\Delta G_{2D}^{\text{terr}} = \frac{\pi \varepsilon^2}{h \Delta \mu}, \quad (1)$$

where ε , h and $\Delta \mu$ are the edge free energy, atomic height and the driving force for growth, respectively. On

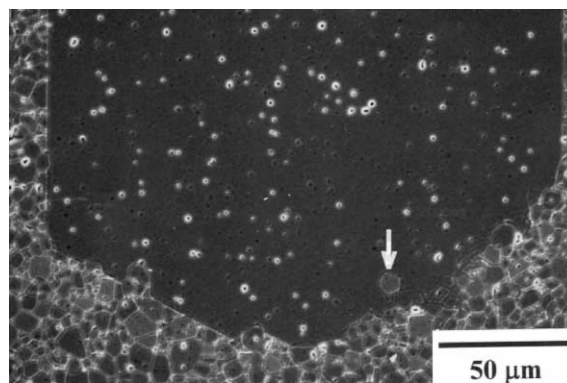


Fig. 2. Scanning electron micrograph of the elongated abnormally grown alumina grain from the specimen shown in Fig. 1(b).

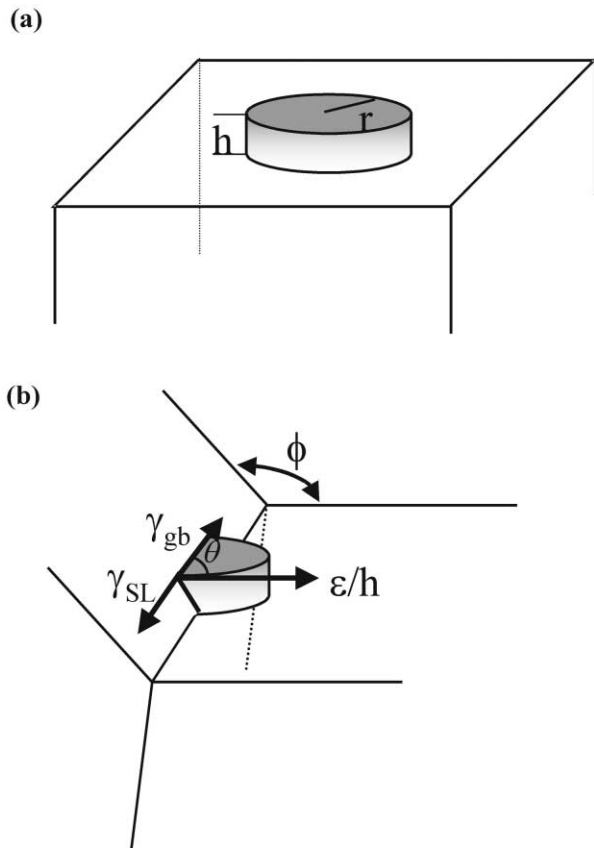


Fig. 3. Schematic diagram of 2-D nucleation; (a) at the terrace and (b) at the re-entrant edge.

the other hand, when 2-D nucleation takes place at the re-entrant edge of an angle ϕ (radians), the barrier is expressed as

$$\Delta G_{2D}^{\text{edge}} = \Delta G_{2D}^{\text{terr}} \left(\frac{\theta - \cos\theta \sin\theta}{\pi} - \frac{\sin\theta}{\pi \tan\phi} \frac{h}{r} \right), \quad (2)$$

where r and θ (radians) are the radius of the critical 2-D nucleus and the contact angle of the nucleus with the edge, respectively. When the re-entrant edge angle ϕ is $\pi/2$, the second term in the parenthesis of Eq. (2) is zero. In that case, the nucleation barrier on the re-entrant edge is reduced by 50 and 90% from that on the terrace, respectively, for $\theta = \pi/2$ and $\pi/4$.

It is indeed well established in the crystal growth field that twin plane re-entrant edge (TPRE) provides a favorable site for growth.³⁹ A similar role is expected for grain boundary re-entrant edge (GBRE), which may explain how the partially wetted non-basal plane migrates much faster than that of the fully wetted flat basal plane. In this respect, the elongated abnormal grains in Figs. 1 and 2 can be explained in terms of a growth by homogeneous like 2-D nucleation process of flat basal plane and by heterogeneous like 2-D nucleation process of non-basal planes. Grain entrapment shown in Fig. 2 is a consequence of rapid growth of non-basal planes. Such

grain entrapment due to GBRE has also been observed recently in TaC–TiC–Ni system.³⁰

4. Conclusion

AGG occurred in alumina with locally presenting small amount of liquid was investigated. A few grains were observed to grow extensively and anisotropically at the region where the liquid content is very limited. The migration rate of partially wetted non-basal planes was much higher than that of fully wetted basal plane. AGG behavior in alumina has been explained in terms of 2-D nucleation and lateral growth mechanism. In that case, the formation of the grain boundary may significantly enhance the migration rate of interface because the nucleation becomes much easier at the re-entrant edges. In alumina, therefore, the non-basal surface with high frequency of grain boundaries can grow much faster than the fully wetted basal surface.

Acknowledgements

This work was supported by the Ministry of Science and Technology of Korean Government through Creative Research Initiatives. Discussions with Professor Duk Yong Yoon were very helpful.

References

1. Park, C. W. and Yoon, D. Y., Effects of SiO₂, CaO and MgO additions on the grain growth of alumina. *J. Am. Ceram. Soc.*, 2000, **83**(10), 2605–2609.
2. Shaw, N. J. and Brook, R. J., Structure and grain coarsening during the sintering of alumina. *J. Am. Ceram. Soc.*, 1986, **69**(2), 107–110.
3. Gavrilov, K. L., Bennison, S. J., Mikeska, K. R. and Levi-Setti, R., Grain boundary chemistry of alumina by high-resolution imaging SIMS. *Acta Mater.*, 1999, **47**(15), 4031–4039.
4. Bennison, S. J. and Harmer, M. P., Grain growth kinetics for alumina in the absence of a liquid phase. *J. Am. Ceram. Soc.*, 1985, **68**(1), C22–C24.
5. Bae, S. I. and Baik, S., Abnormal grain growth of alumina. *J. Am. Ceram. Soc.*, 1997, **80**(5), 1149–1156.
6. Song, H. and Coble, R. L., Morphology of platelike abnormal grains in liquid-phase sintered alumina. *J. Am. Ceram. Soc.*, 1990, **73**(7), 2086–2090.
7. Kim, Y.-M., Hong, S.-H. and Kim, D.-Y., Anisotropic abnormal grain growth in TiO₂/SiO₂-doped alumina. *J. Am. Ceram. Soc.*, 2000, **83**(11), 2809–2812.
8. Bae, S. I. and Baik, S., Sintering and grain growth of ultra pure alumina. *J. Mater. Slid.*, 1993, **28**, 4197–4204.
9. Bateman, C. A., Bennison, S. J. and Harmer, M. P., Mechanism for the role of MgO in the sintering of alumina containing small amounts of a liquid phase. *J. Am. Ceram. Soc.*, 1989, **72**(7), 1241–1244.
10. Simpson, Y. K. and Carter, C. B., Faceting behavior of alumina in the presence of a glass. *J. Am. Ceram. Soc.*, 1990, **73**(8), 2391–2398.

11. Kaysser, W. A., Sprissler, M., Handwerker, C. A. and Blendell, J. E., Effect of a liquid phase on the morphology of grain growth in alumina. *J. Am. Ceram. Soc.*, 1987, **70**(5), 339–343.
12. Powell-Dogan, C. A. and Heuer, A. H., Microstructure of 96% alumina ceramics: I, characterization of the as-sintered materials. *J. Am. Ceram. Soc.*, 1990, **73**(12), 3670–3676.
13. Kolar, D., Discontinuous grain growth in multiphase ceramics. In *Ceramics Transactions. Vol. 7, Sintering of Advanced Ceramics*, ed. C. A. Handwerker, J. E. Blendell and W. A. Kaysser. Am. Ceram. Soc., Westerville, OH, 1990, pp. 529–545.
14. Schreiner, M., Schmitt, T., Lassner, E. and Lux, B., On the origin of discontinuous grain growth during liquid phase sintering of WC–Co cemented carbides. *Powder Metall Int.*, 1984, **16**(4), 180–183.
15. Choi, K., Hwang, N. M. and Kim, D.-Y., Effect of VC addition on the microstructural evolution of WC-Co alloy: mechanism of grain growth inhibition. *Powder Metall*, 2000, **43**(2), 168–172.
16. Hennings, D. F. K., Janssen, R. and Reynen, P. J. L., Control of liquid phase enhanced discontinuous grain growth in barium titanate. *J. Am. Ceram. Soc.*, 1987, **70**(1), 23–27.
17. Yoo, Y.-S., Kim, H. and Kim, D.-Y., Effect of SiO₂ and TiO₂ addition on the exaggerated grain growth of BaTiO₃. *J. Eur. Ceram. Soc.*, 1997, **17**(80), 805–811.
18. Kang, S.-J. L. and Han, S.-M., Grain growth in Si₃N₄-based materials. *Mater. Res. Bull.*, 1995, **20**(2), 33–37.
19. Rhee, S.-H., Lee, J. D. and Kim, D.-Y., Effect of heating rate on the exaggerated grain growth behavior of β-Si₃N₄. *Mater. Lett.*, 1997, **32**, 115–120.
20. Heuer, A. H., Fryburg, G. A., Ogbuji, L. U., Mitchell, T. E. and Shinozaki, S., β–α Transformation in polycrystalline SiC: I. Microstructural aspects. *J. Am. Ceram. Soc.*, 1978, **61**(9), 406–412.
21. Hong, S. H. and Messing, G. L., Anisotropic grain growth in diaphasic-gel derived titania-doped mullite. *J. Am. Ceram. Soc.*, 1998, **81**(5), 1269–1277.
22. Prochazka, S., Dole, S. L. and Hejna, C. I., Abnormal grain growth and microcracking in boron carbide. *J. Am. Ceram. Soc.*, 1985, **68**(9), C235–C236.
23. Yoon, D. N. and Huppmann, W. J., Grain growth and densification during liquid phase sintering of W–Ni. *Acta Metall*, 1979, **27**, 693–698.
24. Oh, U.-C., Chung, Y.-S., Kim, D.-Y. and Yoon, D. N., Effect of grain growth on pore coalescence during the liquid-phase sintering of MgO–CaMgSiO₄ systems. *J. Am. Ceram. Soc.*, 1988, **71**(10), 854–857.
25. Yoon, H.-H. and Kim, D.-Y., Effect of heating rate on the exaggerated grain growth during the sintering of Sr-hexaferrite. *Mater. Lett.*, 1994, **20**, 293–297.
26. Park, Y. J., Hwang, N. M. and Yoon, D. N., Abnormal grain growth of faceted (WC) grains in a (Co) liquid matrix. *Metall. Mater. Trans., A*, 1996, **27A**, 2809–2819.
27. Kwon, S.-K., Hong, S.-H., Hwang, N. M. and Kim, D.-Y., Coarsening behaviors of C₃S and C₂S grains dispersed in a clinker melt. *J. Am. Ceram. Soc.*, 2000, **83**(5), 1247–1252.
28. Kang, M.-K., Yoo, Y.-S., Kim, D.-Y. and Hwang, N. M., Growth of BaTiO₃ seed grains by the twin plane re-entrant edge mechanism. *J. Am. Ceram. Soc.*, 2000, **83**(2), 385–390.
29. Oh, K.-S., Jun, J.-Y., Hwang, N. M. and Kim, D.-Y., Shape dependence of coarsening behavior of NbC grains dispersed in a liquid matrix. *J. Am. Ceram. Soc.*, **83**(12), 3110–3120.
30. Choi, K., Choi, J.-W., Kim, D.-Y. and Hwang, N. M., Effect of coalescence on the grain coarsening during liquid-phase sintering of TaC–TiC–Ni cermets. *Acta Mater.*, 2000, **48**, 3125–3129.
31. Herring, C., Effect of change of scale on sintering phenomena. *J. Appl. Phys.*, 1950, **21**, 301–303.
32. Wynblatt, P. and Gjostein, N. A., Particle growth in model supported metal catalysts — I. Theory. *Acta Metall.*, 1976, **24**, 1165–1174.
33. Wynblatt, P., Particle growth in model supported metal catalysts — II. Comparison of experiment with theory. *Acta Metall.*, 1976, **24**, 1175–1182.
34. Kooy, C., Anisotropic exaggerated grain growth and sintering in MnFe₂O₄ and Y₃Fe₅O₁₂. In *Science of Ceramics*, Vol. 1., ed. G. H. Stewart. Academic Press, New York, 1962, pp. 21–34.
35. Jackson, K. A., Interface structure. In *Growth and Perfection of Crystals*, ed. R. H. Doremus et al. John Wiley, New York, 1958, pp. 319–324.
36. Shaw, T. M. and Duncombe, P. R., Forces between aluminum oxide grains in a silicate melt and their effect on grain boundary wetting. *J. Am. Ceram. Soc.*, 1991, **74**(10), 2495–2505.
37. Kim, J.-J. and Harmer, M. P., Infiltration of glass melt into fully dense Al₂O₃ and MgO ceramics. *J. Am. Ceram. Soc.*, 1998, **81**(1), 205–208.
38. Flaitz, P. L. and Pask, J. A., Penetration of polycrystalline alumina by glass at high temperatures. *J. Am. Ceram. Soc.*, 1987, **70**(7), 449–455.
39. Howe, J. M. Crystal growth from the liquid. In *Interfaces in Materials*. John Wiley & Sons, New York, 1997, pp. 256–268.